Multimedia Tools and Applications (2025) 84:27963–27985
https://doi.org/10.1007/s11042-024-20269-w

A computer-vision based framework for virtual 3D garment reconstruction

Ying Dang[1] · Tao Ruan Wan[2] · Long Xi[3] · Wen Tang[4]

Received: 2 November 2022 / Revised: 22 August 2024 / Accepted: 11 September 2024 /
Published online: 24 September 2024

Abstract
Existing 3D garment reconstruction methods are difficult to implement for online fashion design and e-commerce or special applications. This paper proposes a novel computer-vision framework for 3D garment digital reconstruction, which aims to reconstruct high-quality and realistic virtual 3D garments with fabric mechanic properties for 3D virtual try-on. The new segmentation scheme is proposed to separate the 3D garment point clouds from background points, which is suitable for 3D human shapes and is adaptive for different 3D garment models in different scenes. The new Statistical Outlier Removal algorithm and the learning-based method PointCleanNet are combined to remove noise and outliers in 3D garment point clouds, which provides high-fidelity and high-quality 3D garment point clouds. The 3D garment meshes are then reconstructed from their corresponding point clouds with a modified rolling ball algorithm. Finally, the meshes are improved and converted into physics-based virtual try-on 3D garments with fabric mechanic properties added, which enables the assessment of different body shapes with varied sizes for the same reconstructed 3D garment. Comparison experiments demonstrate that our framework achieves high-quality and realistic 3D garment reconstruction and accurate 3D virtual try-on from 2D garment images. We also demonstrate the proposed framework on a large range of various garments to show this approach has a great potential for garment future technology, such as online garment shopping, garment design and manufacturing.

Keywords 3D point cloud · Multi-view images · 3D reconstruction · Virtual garment

✉ Tao Ruan Wan
t.wan@bradford.ac.uk

Ying Dang
yydspn@163.com

Long Xi
lxi@xpu.edu.cn

Wen Tang
wtang@bournemouth.ac.uk

1 Department of Technology, Yan'an Open University, Shaanxi Yan'an 716000, China

2 Faculty of Engineering & Digital Technologies, University of Bradford, Bradford BD7 1DP, UK

3 Shaanxi Key Laboratory of Clothing Intelligence, School of Computer Science, Xi'an Polytechnic University, Xi'an 710048, Shaanxi, China

4 Department of Creative Technology, Bournemouth University, Bournemouth BH12 5BB, UK

1 Introduction

Computer vision-based methods have advanced 3D garment reconstruction techniques.The 3D information can be obtained via several images of a garment, which in turn can be used to automatically reconstruct the full 3D digital garment based on point cloud methods. Recently, 3D digital reconstruction using dense 3D point clouds has shown some potential practical applications [57]. 3D Digital garments are important forms of digital assets to the evolution of the digital development of the world and can be used in countless applications, including computer animation, digital museums [31], digital games [41] [54], online shopping, culture conservation, virtual try-on [14] and personalized garment design [22]. 3D garment reconstruction is one of the key technologies for obtaining digital garments.

To achieve 3D digital design and garment reconstruction, the design of a garment that mainly consists of sketches or drawings and contours are adjusted to ensure the 3D reconstruction is a true representation of the designer's original design ideas. The current state-of-the-art 3D garment reconstruction approaches [10, 53] utilized digital printing, flat pleating and garment tailoring on 3D models. This process of 3D garment reconstruction demands experienced technicians to manually construct realistically [5, 26, 32, 49]. Moreover, these methods are difficult to implement for online fashion design and e-commerce or special applications. For example, historical fashion pieces in museums do not allow direct contact measurement for accurate 3D reconstructions for digital preservation. Thus, our motivations for the proposed computer-vision based framework are aimed to reconstruct high-quality and realistic virtual 3D garments with fabric mechanic properties that can be directly applied to the virtual try-on for the same reconstructed 3D garment, enabling the assessment of different body shapes with varied sizes. Our framework does not need hand-crafted measurements and is easy to use for the general purpose of digital garment creation.

To develop the framework for the general purpose of digital garment generation, we choose mobile phone cameras to capture a set of garment images from multiple views (multi-view images), which imposes several technical challenges, such as processing a large number of images with fixed angle intervals as well as dealing with varied light conditions. The 3D point cloud scene is extracted from the captured garment images using the structure-from-motion (SFM) algorithm [34]. Since the extracted 3D point cloud scene consists of the 3D garment, background and noisy points, we employ 3D point cloud segmentation and de-noising algorithms to separate the 3D garment point cloud from the background and noisy points, which can produce high-quality garment meshes suitable for the virtual try-on garment requirements. The novelty of our 3D garment segmentation is to separate the 3D garment from the background points on different 3D garment models by applying the combination of the cylindrical segmentation algorithm [40] and the Euclidean clustering algorithm [40]. The Statistical Outlier Removal algorithm [40] and the learning-based method PointCleanNet [39] are used to remove outliers and noisy points in 3D garment point clouds. The 3D garment meshes are reconstructed from 3D garment point clouds using the modified rolling ball algorithm, and these modifications improve the mesh surface continuity during the reconstruction. The hole-close algorithm is used to recover the missing data of the reconstructed 3D garment mesh surface to obtain high-quality and realistic 3D garment meshes. The texture generation method can generate reali stic fabric mechanic properties for 3D garment meshes. Finally, we demonstrate our virtual try-on performed on different 3D garment models. The detailed illustration of the proposed framework is explained in Section 3. Section 4 illustrates the comparison experiments, including 3D garment point cloud extraction from images (Section 4.1), 3D garment point cloud segmentation(Section 4.2), outlier removal and de-noising for 3D

garment point cloud(Section 4.3), 3D garment mesh surface synthesis(Section 4.4) and 3D garment virtual try-on(Section 4.5). Section 5 gives a brief summary of the achievements, comparison results, limitations and future works.

To the best of our knowledge, our computer-vision based framework is the first attempt of its kind to achieve the 3D garment reconstruction and 3D virtual try-on from 2D garment images.

The main contributions of this paper are:

- A novel computer-vision framework for 3D garment digital reconstruction is proposed, which consists of 3D garment point cloud extraction, segmentation, de-noising, 3D mesh surface reconstruction and virtual try-on.
- The combination of the cylindrical segmentation algorithm and the Euclidean clustering algorithm is used to separate the 3D garments from the background points on different 3D garment models, which produces high-quality garment meshes suitable for the virtual try-on garment requirements.
- The modified rolling ball algorithm and hole-close are introduced to recover the missing data of the reconstructed 3D garment mesh surface for obtaining high-quality and realistic 3D garment meshes.
- The virtual garment try-on application based on our proposed framework has been developed on different 3D human models with different sizes of 3D garment models.

2 Related work

2.1 3D garment reconstruction

With the in-depth development of digitization in the garment and textile industry, some approaches [3, 10, 46, 52, 52] focusing on the 3D garment reconstruction have been proposed. Fang [10] proposes a garment piece construction method based on sketch drawing for the interactive design of the garment piece, which processes the contour line of the garment piece and enriches the styles of the garment model. Umetani [46] develops a garment design tool for garment interactive modelling and editing, which obtains special effects of the garment model after virtual stitching and displays the 3D garment effectively. Geometric modeling [52] generates garment models through the changes of various geometric topological structures on the mesh surface of the 3D model. Wei [52] proposes a garment generation algorithm based on style maintenance, which generates a 3D model that maintains the original style and fits the human model. Brouet [3] implements the deformation of various parts of the garment model by adjusting the vertices of the garment pieces, but it requires a large amount of vertex information to store and calculate dynamic garment behaviours [55].

3D garment models can also be reconstructed from binocular and monocular multi-view 2D images. Binocular multi-view reconstruction needs to maintain multiple cameras at a fixed distance during the operation, which requires complex operations and powerful (expensive) devices for stereo visions. Monocular multi-view reconstruction operates with limited processing resources and simple operations. Pan [35] optimizes the image matching process in monocular multi-view 3D reconstruction to reduce the time on feature point matching and improve the quality of the reconstructed 3D point cloud. Hu [21] proposes a Scale Invariant Feature Transform (SIFT) algorithm for feature point detection and matching, which extracts

contour information through Mask R-CNN to separate the 3D garment from the background and uses Poisson to reconstruct the 3D garment.

Xu [51] developed a web-based design support system that enables users to design realistic and interesting skirts in the form of technical sketches over the internet. Compared with traditional computer-aided design (CAD) systems, the proposed system is more effective and easier to operate as users can create technical sketches in accurate proportions with simple computer operations in a few mouse clicks. He [16] proposed Sketch2Cloth, a sketch-based 3D garment generation system that uses the unsigned distance fields from the user's sketch input. Sketch2Cloth first estimates the unsigned distance function of the target 3D model from the sketch input and then extracts the mesh from the estimated field with Marching Cubes. Chen [4] introduced a novel baseline approach for sketch-based garment reconstruction using an end-to-end generative network capable of generating garment models from single hand-drawn sketches. Hu [20] designed a novel pipeline to obtain 3D high-quality textile models based on KinectFusion. The accuracy and robustness of KinectFusion are improved via a turntable. Experimental results show that the proposed method can conveniently reconstruct a three-dimensional textile model with synthesized texture. Kuzmichev [25] proposed a new method of virtual reconstruction of an RH that is based on automatic consideration of all joining elements. The purpose of this paper is to apply 2D and 3D existing CAD for virtual reconstruction of the very specific kind of women's garments such as a side-saddle riding habit (RH) used in 1875-1915. This study should help researchers and practical specialists to recreate and save the historical treasure in a digital way. Špelic [36] aims to present a significant usage of computer-aided design (CAD)/computer-aided manufacturing (CAM) systems in the apparel and textile industry. The paper makes clear that although this technological concept is rather old, the use of the CAD/CAM systems will inevitably broaden in terms of applicability to garment new production stages.

This paper is based on the most accessible RGB cameras on a mobile phone to obtain multi-view garment images from which to construct a 3D point cloud scene. Background, noise and outliers are common in the extracted 3D point cloud scene captured by an RGB camera due to the luminance, caption angles and distances. Thus, the 3D point cloud segmentation and de-noising are required to separate the 3D garment point cloud from background, noise and outliers.

2.2 3D reconstruction from point clouds

3D point cloud segmentation methods [11, 23, 58] can be divided into two categories according to the organized and disordered input 3D point cloud data [45]. For organized 3D point clouds, Zhu [58] proposes a point cloud segmentation algorithm based on scan lines for large scenes. However, this method is sensitive to noise and uneven or sparse 3D point clouds [15]. For disordered 3D point clouds, it mainly includes area growth [23], clustering [56] and model fitting [11]. Area growth [23] is susceptible to noise [1]. The clustering segmentation algorithm [56] segments 3D point clouds that contain the same attributes, which shows slow convergence and low efficiency [44]. The model fitting method Random Sample Consensus (RANSAC) [56] directly operates on unorganized 3D point clouds generated by 3D laser scanning and can be used to segment planes accurately, which takes less time than area growth [23] and clustering [56] and can be considered the most advanced technology for model fitting. Some methods based on RANSAC have been improved, such as the cylindri-

cal segmentation algorithm [40] and the Euclidean clustering segmentation algorithm [40], improving the accuracy of the segmentation. In this paper, we use the well-known algorithm RANSAC to extract mathematical features, such as straight lines and circles, for 3D garment point clouds.

Cruz et al. [28, 47, 48] propose de-noising algorithms for 3D point cloud based on surface fitting [28], Laplace distribution [48] and normal vector distance estimation [47]. However it shows lower de-noising performance since the manually made features are not efficient for the de-noising. Recent emerged deep-learning methods [6, 18, 19, 29] extract features automatically and achieve higher performance on de-noising. A de-noising algorithm based on non-local enhanced convolutional neural networks [47] and a Signoroni grid de-noising algorithm [29] have been proposed to achieve effective de-noising. Although these algorithms deal with large-scale noise and complex point cloud models, they are limited to large and dense 3D point clouds with different noise scales. We use a statistical outlier removal filter [40] with a deep learning-based PointCleanNet algorithm [39] together to achieve effective and robust removal of noise and outliers, which handles large and dense 3D point clouds with noise and outliers at different scales.

Mesh surface reconstruction [43, 50]restores the object surface of the 3D point cloud. 3D mesh surface reconstruction can be divided into two parts, including surface fitting [12] and mesh reconstruction [9]. Surface fitting reconstruction is suitable for surfaces with smooth surfaces and small changes, which is challenging to achieve surface objects with complex topology [59]. Mesh reconstruction reconstructs the triangular mesh model and describes the topology of complex objects [59], which is widely used in point cloud surface reconstruction. Greedy Projection Triangulation (GPT) [30] reconstructs the 3D point cloud obtained from LiDAR sensors with 3D geographic information. Although the greedy projection triangulation reconstruction algorithm can completely restore the mesh surface, the resulting surface is not smooth and has many holes.

Hoppe [17] proposes a Poisson mesh surface reconstruction algorithm, which over-smooths the 3D mesh model and loses detailed information of 3D meshes. Bernardini [2] proposes the Ball Pivoting Algorithm algorithm for grid reconstruction of dense point clouds, which is time efficient for 3D reconstruction, but there are some holes in the reconstructed meshes. This paper compares the Poisson reconstruction, GPT and rolling ball reconstruction algorithms for the 3D garment reconstruction and chooses the rolling ball reconstruction based on the reconstruction results. Finally, the holes are completed using the hole-close algorithm [40].

The latest advancements in computer vision technology cover several areas, including deep learning and convolutional neural networks [27], 3D reconstruction and point cloud processing [8], self-supervised learning, object detection and instance segmentation, generative adversarial networks (GANs) [7], as well as augmented reality (AR) and virtual reality (VR). Among these, 3D reconstruction-particularly using point cloud data-has seen remarkable progress with deep learning methods such as [37], PointNet++ [38], and Transformer-based point cloud networks. These methods excel at extracting and processing 3D point cloud data from multi-view images or depth sensors, achieving higher precision in 3D object reconstruction and surface modelling. However, these methods are not suitable for dynamic 3D garments, because the fabric garments are dynamic, soft and deformable. In this paper, our proposed framework achieves high-quality and realistic 3D garment reconstruction and accurate 3D virtual try-on from 2D garment images.

3 Method

Figure 1 shows the computer-vision framework that consists of four modules: a) 3D Point Cloud Reconstruction, b) 3D Point Cloud Segmentation and De-noising, c) Mesh Surface Reconstruction and d) Virtual Try-on. First, the 3D point cloud scenes of the garments are reconstructed from multi-view images. Second, the cylindrical segmentation [40], Euclidean algorithm [40] and Passthrough filter are employed for the separation of the garment from the background, which can be adapted to different shapes of the garments. To achieve high-quality 3D garment models, a combination of a deep-learning PointCleanNet algorithm [39] and a statistical model is used to remove the noise and the outliers for the 3D garment point clouds. Third, the modified rolling ball algorithm [2] is employed to reconstruct the high-quality and realistic 3D garment meshes. The hole-close algorithm [40] is used to recover the missing data of the reconstructed 3D garment mesh surface to obtain high-quality and realistic 3D garment meshes. Finally, we demonstrate the 3D virtual try-on can be performed on different 3D human models with different sizes of 3D garment models. The details of our framework are in the following subsections.

3.1 3D garment scene reconstruction

To obtain the multi-view RGB images, a mobile phone camera is used and located at a fixed distance and different views from the real-world garment model. Multi-view RGB images are captured under optimal lighting conditions without extreme low light and over-exposure for 3D scene reconstruction.

Since the reconstructed 3D scene consists of the 3D garment point cloud, background and noisy points, the 3D point cloud segmentation and de-noising for the reconstructed 3D scene are necessary to separate the 3D garment point cloud from the background and noisy points

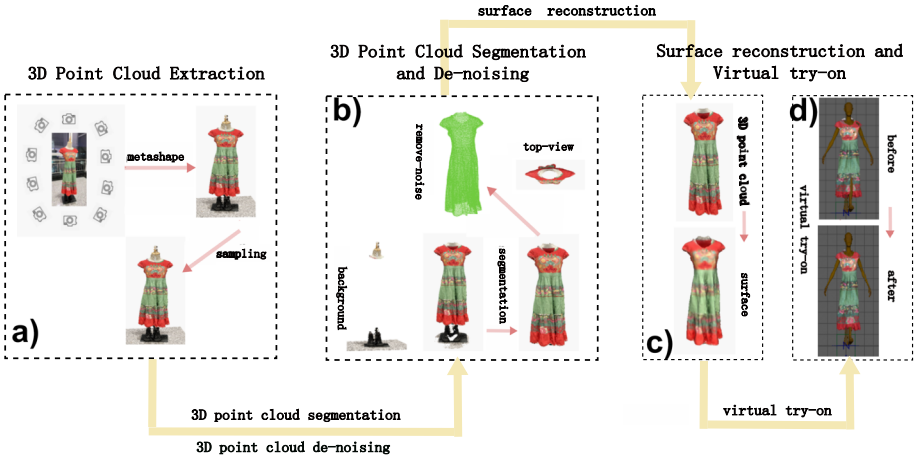

Fig. 1 The proposed computer-vision framework consists of four main modules: a) 3D point cloud extraction, b) 3D point cloud segmentation and de-noising, c) mesh surface reconstruction and d) Virtual try-on

and produce high-quality of cloth meshes suitable for the virtual try-on garment requirements. The reconstructed 3D scene is down-sampled from approximately 300,000 points to about 10,000 points for the low storage and fast calculation in the 3D point cloud segmentation and de-noising to obtain a more realistic 3D garment point cloud.

3.2 3D garment point cloud segmentation

The novelty of our 3D garment segmentation is to combine the cylindrical segmentation algorithm [40] with a Passthrough filtering [40] and an Euclidean clustering algorithm [40] for separating the 3D garment from the background points on different 3D garment models, producing high quality of garment meshes suitable for the virtual try-on garment requirements.

The cylindrical segmentation algorithm [40] is based on the random sampling consistency (RANSAC) algorithm [13] that segments a cylindrical model from a 3D garment point cloud by segmenting a 2D planar model and performing the cylindrical segmentation on the remaining point cloud. First, at least three non-collinear points are randomly selected from the 3D garment point cloud to estimate the 2D plane model by iteratively finding the optimal parameters, as defined by (1). The iterative method iteratively finds the in-office and out-of-office points, where in-office points represent the points that need to be reserved, and out-of-office points are the points that need to be removed. Second, The unit normal vector of each point in the 3D garment point cloud is calculated to create the initial value of the cylinder vertical axis vector $(a0, b0, c0)$ of the 3D cylinder model. The created 3D cylinder model is located on the estimated 2D plane model vertically, which is parallel to the Z axis. Since the 3D garment point cloud is parallel to the Y axis, the $(a0, b0, c0)$ is then transformed to be paralleled with the Y axis, which leads the 3D cylinder model to be vertical to the (X, Z) plan. The parametric equation determines the specific location of the cylinder, as defined by (2).

$$ax + by + cz = d, a^2 + b^2 + c^2 = 1, d > 0 \tag{1}$$

$$\begin{aligned} f = (x - x_1)^2 + (y - y_1)^2 + (z - z_1)^2 - \\ [a\,(x - x_1) + b\,(y - y_1) + c\,(z - z_1)]^2 - r^2 \end{aligned} \tag{2}$$

where $(x1, y1, z1)$ represents the coordinates of the center of the circle, r represents the radius of the cylinder base, (a, b, c) represents the cylinder axis vector.

Finally, the four parameters of normal number, normal weight, 3D cylinder radius and distance from the inner point of the 3D cylinder model to the clothing point cloud are adjusted to create the final 3D cylinder model for different 3D garment models.

According to the difference of the 3D garment model, the passthrough filtering is combined with the cylindrical segmentation to separate the different 3D garment point clouds (e.g. skirts, trousers) from background points. First, a 3D bounding box is formulated by (3). Second, the passthrough filter changes y_{min} and y_{max} to keep and discard points along the Y axis.

$$P = \{p_i \| \text{Min} \leq p_i \leq \text{Max}\} = \begin{cases} x_{\min} \leq x_i \leq x_{\max} \\ y_{\min} \leq y_i \leq y_{\max} \\ z_{\min} \leq z_i \leq z_{\max} \end{cases} \tag{3}$$

where $p_i \in \{x_i, y_i, z_i\}$. $(x_{\min}, y_{\min}, z_{\min})$ and $(x_{\max}, y_{\max}, z_{\max})$ are the minimum and maximum values along the X, Y and Z directions.

The combination of cylindrical segmentation algorithm [40] and Euclidean clustering algorithm [40], as defined by (4), separates the upper body clothing area and floor.

After the cylindrical segmentation, a point x_i is randomly selected from the remaining points to find K nearest points by using a Kd-Tree through a threshold of an Euclidean distance dL, as defined by (4).

$$dL = \sqrt{\sum_{i=1}^{n} (x_i - y_i)^2}. \tag{4}$$

where x_i represents a randomly selected point, y_i represents the nearest point in K nearest points.

The selected K nearest points need to be further grouped by finding the K_2 points where the Euclidean distance between pi and K nearest points is less than a fixed threshold. Finally, K_2 points are reserved, and other points are removed.

3.3 3D point cloud de-noising

To remove the noise and outliers in 3D garment point clouds, a Statistical Outlier Removal filter [40] and a deep learning-based PointCleanNet [39] are combined to further obtain a realistic 3D garment point cloud, which is effective and robust to noise and outliers.

The Statistical Outlier Removal filter [40] calculates the average Euclidean distance d_{ij} from each point in the input 3D garment point cloud. If $d_{ij} > T$, as defined by (5), (6) and (7), the corresponding points are considered as outliers and need to be eliminated. Vice versa.

$$\mu = \frac{1}{nk} \sum_{i=1}^{m} \sum_{j=1}^{k} d_{ij} \tag{5}$$

$$\sigma_d = \sqrt{\frac{1}{nk} \sum_{i=1}^{m} \sum_{j=1}^{k} \left(d_{ij} - \mu\right)^2} \tag{6}$$

$$T = \mu + \alpha \cdot \sigma_d \tag{7}$$

where $i = (1, ..m)$ represents a total of m points, $j = (1, ...k)$ represents k neighbour points. μ represents mean distance. σ_d represents the standard deviation of distance. d_{ij} represents the Euclidean distance from each point to its neighbours. T represents the threshold. α is the standard deviation multiplier and varies from each 3D garment.

The PointCleanNet algorithm is based on the PCPNet [13], which estimates the displacement vectors for each point and projects noisy points onto the original clean surfaces. The 3D point clouds P_i, including the noisy points, are given as input for 1D convolutions and space transfer network (STN) to extract the point-wise features $h(p_j)$ of each point p_j and aggregate all features to the global features H, as defined by (8). The per-point displacement vectors di considered as the translation are estimated from the global features to translate

each point onto the original clean surfaces, as defined by (9).

$$H\left(P_i\right) = \sum p_j \in P_i h\left(p_j\right). \tag{8}$$

$$P_{output} = p_i + d_i \tag{9}$$

The loss function for PointCleanNet focuses on minimizing the L_2 distance between the output cleaned 3D point cloud P_{output} and the ground-truth clean 3D point cloud, as defined by (10), (11) and (12).

$$L_s\left(\tilde{p}_i, P_{\tilde{p}_i}\right) = \min_{p_j \in P_{\tilde{p}_i}} \left\| \tilde{p}_i - p_j \right\|_2^2 \tag{10}$$

$$L_l\left(\tilde{p}_i, P_{\tilde{p}_i}\right) = \max_{p_j \in P_{\tilde{p}_i}} \left\| \tilde{p}_i - p_j \right\|_2^2 \tag{11}$$

$$L_\alpha = \alpha L_s + (1-\alpha) L_l \tag{12}$$

Since the PointCleanNet [39] requires 3D point cloud data without texture, we add texture to the 3D garment point cloud for 3D garment mesh surface reconstruction.

3.4 3D garment mesh surface reconstruction

Once the clean 3D garment point cloud is obtained, a modified rolling ball method (BPA) [2] is used to reconstruct the mesh of the garment surface.

First, a ball is dropped onto the 3D point cloud and the ball will get caught and settle upon three points to form a seed triangle, which becomes part of the 3D mesh. Second, from the seed triangle, the ball pivots along the seed triangle edge formed from two points. The ball then settles in a new location where a new triangle is formed from two of the previous points and one new point. Third, as we continue rolling and pivoting the ball, new triangles are formed and added to the mesh. Finally, the ball continues rolling until the 3D mesh is fully formed. Most importantly, the BPA algorithm preserves the opening surfaces in the upper and bottom areas of garments during the mesh surface reconstruction.

The BPA [2] is modified from two aspects for clean 3D garment point clouds. Firstly, if the points are too far apart and the ball falls through between points, we check that the normal of the new triangle facet is consistently oriented with the point's normals. If it is not, the triangle is rejected. Secondly, if the surface has creases and the ball is larger than these creases, the ball will roll over the creases and ignore the points inside the creases. To fix this, multiple ball radii are used in the modified BPA. The smaller balls roll into these creases and the larger balls prevent the fall through for improving the surface continuity.

To obtain high-quality garment mesh surfaces, we complete the holes in the reconstructed surfaces. Specifically, the broken edges are found and considered as the holes in the 3D garment mesh. For each hole, the broken edges defined as the half-edges are sorted by finding the two half-edges with the same normal vector. For the two half-edges with the same normal vector, the third edge is added to form a new triangular patch. By iterating this process, all holes are completed.

4 Experiment

Four experiments are conducted to prove the feasibility and generality of the framework. First, we obtained clothing point cloud data using a multi-view approach and extracted six different 3D garment point clouds using cylindrical segmentation, Euclidean clustering segmentation, and Passthrough filtering algorithms.

Second, the Statistical Outlier and PointCleanNet [39] algorithms are applied to remove outliers and noisy points on segmented 3D garment point clouds. Third, we compare Poisson reconstruction, greedy triangulation algorithms and rolling ball algorithm on 3D mesh surface reconstruction and employ the modified rolling ball algorithm to reconstruct the high-quality and realistic 3D garment mesh surface. Finally, we perform a dynamic physical simulation of the 3D garment on the virtual model and show our virtual try-on on different 3D garment models.

4.1 3D garment point cloud extraction form images

We extract 3D garment point clouds from real-life 3D models wearing six different garments, including a red dot, a dress, a short sleeve, a denim jacket, a long pant and a short skirt. First, we use the mobile phone camera to capture more than 150 2D images of each real-life 3D model from a fixed distance with different angles between 0 and 45 degrees. Second, the six types of dense 3D garment point clouds are extracted from the captured images, as shown in Fig. 2.

COLMAP [33] is a reconstruction method that can be applied to any scene. For images taken from different angles, the optimal angle can be found to improve the effectiveness of reconstruction and its accuracy. The completeness of the reconstruction model can be improved through triangulation methods and beam adjustment algorithms. Figure 3 shows the comparison between the SFM-MVS method in our framework with the COLMAP reconstruction method, The experiments show that the point cloud reconstructed by our proposed SFM-MVS compared with COLMAP generated clearer surface textures, reduced noisy points and holes on the garment surface, making it suitable to segment the garment from the

Fig. 2 Six different dense 3D garment point clouds for a red dot, a dresses short sleeve, a denim jacket, a long pant and a short skirt

Fig. 3 Comparison diagram of dense reconstruction of 3D garment point cloud experiment

background point cloud and achieve subsequent garment surface reconstruction and virtual fitting to fully display the garment contour structure. The performance is shown in Table 1. Figure 3 also shows the visual comparison of the results generated by the two methods. The SFM-MVS method has a shorter running time and higher efficiency. The point clouds reconstruction results of COLMAP and SFM-MVS for 6 types of garments are shown in Fig. 4.

The extracted 3D garment point clouds are downsampled from about 300,000 points to about 10,000 points for low storage and fast computation in subsequent 3D point cloud segmentation and de-noising, as shown in Table 2.

4.2 3D garment point cloud segmentation

In this experiment, we extract 3D garment point clouds using cylindrical segmentation, Euclidean clustering and Passthrough filter algorithms.

We use cylindrical segmentation to segment red dots skirts, short-sleeved denim jackets, dresses, short skirts and long pants, as shown in Fig. 5. However, the segmentation results show that the cylindrical segmentation removes the useful points on the pants and destroys the integrity of the pants. In addition, cylindrical segmentation does not remove the points on

Table 1 Comparison of the performance of the proposed method with COLMAP

Method	Number of point clouds	Run time(s)
$SFM + WVS$	276657	37
COLMAP	237485	45

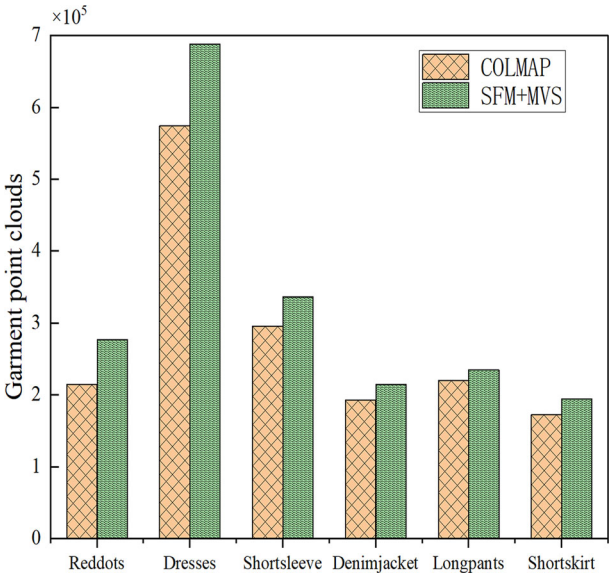

Fig. 4 The horizontal axis represents 6 examples in the instance, and the vertical axis represents the number of reconstructed point clouds. It can be seen that in the six instances, SFM-MVS generated more dense point clouds than COLMAP, indicating more complete reconstructions

Table 2 Six 3D garment point clouds down-sampling

Garments	Initial point	After sampling
Red dots	276657	10799
Dresses	688449	9996
Short sleeve	335781	10976
Denim jacket	214636	10369
Long pants	235075	10535
Short skirt	194318	11031

Fig. 5 Cylindrical segmentation results for the red dot skirt, the short-sleeve, the denim jacket, the dress, the short skirt and the long pant

Fig. 6 Results of the cylindrical segmentation, Euclidean clustering segmentation and Passthrough for six different garments

the model wearing the skirt and cannot completely split the skirt from the background points. To this end, the short skirts and pants are segmented using the combination of the cylindrical segmentation algorithm and the Passthrough filter. The red dots skirts, short-sleeved denim jackets, dresses, short skirts and long pants are segmented using the combination of cylindrical segmentation algorithm and Euclidean clustering, as shown in Fig. 6. We change the following parameters to obtain the four types of 3D garments (red dots, dresses, short sleeves and denim jackets), as shown in Table 3. We also obtain two types of 3D garment point clouds (long pants and short skirts) by changing the parameters of the passthrough filter, as shown in Table 4.

4.3 Outlier removal and de-nosing for 3D garment point cloud

Since the segmented 3D garment point clouds contain outliers and noise, as shown in Fig. 6.

In this experiment, we use Statistical Outlier Removal to remove the outliers of the segmented 3D garment point cloud, as shown in Fig. 7. For noise removal, we follow PointCleanNet and train the network on 18 different shapes (e.g. Stanford bunny, dragon and etc.). We then fine-tune the trained network on the six segmented 3D garment point clouds. The PointCleanNet algorithm estimates the displacement vector of each point and projects the noise point onto the original clean surface, as shown in Fig. 8. The batch size, epoch and learning rate for PointCleanNet are 64, 2000 and 0.00000001, respectively.

To show the complete and real 3D garment, we add the texture of each point after removing the noisy points by PointCleanNet, as shown in Fig. 9.

Table 3 Parameters for 3D point cloud cylindrical segmentation

garments	Normals	Weight	Distance	Radius
Red dots	100	0.18	0.85	0,2
Dresses	80	0.11	1.30	0,4
Short sleeve	100	0.17	0.55	0,2
Denim jacket	100	0.13	0.40	0,2

Table 4 Passthrough filter parameters for 3D garment point cloud segmentation

garments	SetFilterField	SetFilterLimits
Long pants	y	−10,1.4
Short skirt	y	−5,0.8

Fig. 7 Comparison experiments for outlier removel. The outliers shown in red circle are removed

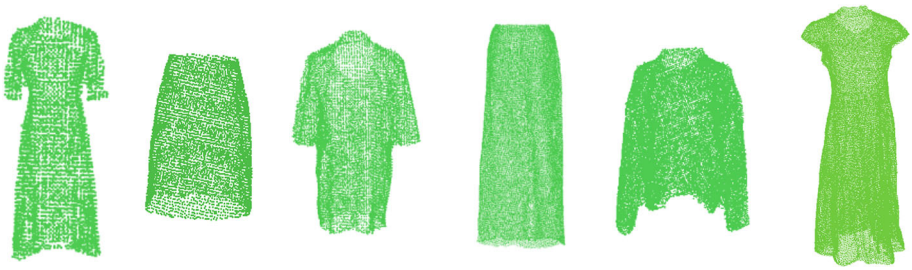

Fig. 8 De-noising results of the PointCleanNet algorithm for six 3D garment point clouds

Fig. 9 The texture for each 3D garment point cloud is added after de-noising

4.4 3D garment mesh surface synthesis

To obtain high-quality garment mesh surfaces from the clean 3D garment point cloud, we compare three mesh surface reconstruction algorithms, including greedy projection triangulation [30], Poisson reconstruction [24] and the modified rolling ball method. These methods are applied to six types of garments, as shown in Fig. 11. The greedy projection triangulation algorithm [30] restores the original shape of the 3D point cloud, but the triangular patches on the surface of the reconstructed clothing model are undulating, and the clothing pieces are not smooth enough. The uniform quality of the Poisson-reconstructed mesh [24] is better than the greedy projection triangulation algorithm [30], and the original folds of the garments are well preserved, but this method automatically fills holes in the opening collar and bottom and over-smoothing at the edges. The modified rolling ball algorithm used in this paper combines the advantages of greedy projection triangulation and Poisson reconstruction. The triangular mesh is uniformly distributed and the surface is smooth, as shown in Fig. 10. The reconstruction triangle number and reconstruction time are reported in Table 5 based on the

Fig. 10 The mesh experiment diagram shows the reconstruction of the rolling ball algorithm

Table 5 3D mesh surface reconstruction results

Experiments	Points	Triangle number	Time-consuming to rebuild(s)
GPT	3000	6475	37
Poisson	3000	6215	40
Rolling ball	3000	6531	30

same 3000 points for each reconstruction method, which indicates that the modified rolling ball algorithm is more time efficient and the number of reconstructed triangular meshes is also larger. More importantly, this method retains the original shape of the 3D garment point cloud, and the opening areas are well preserved, as shown in Fig. 11.

Fig. 11 Comparison experiments between the rolling ball algorithm, greedy projection triangulation and poisson reconstruction for the 3D garment mesh surface reconstruction

The experimental results show that the modified rolling ball algorithm performs better on 3D garment mesh surface reconstruction. Compared with the clothing prototype, the rolling ball method restores a high-quality 3D garment mesh surface, which provides a realistic 3D garment mesh surface for the virtual try-on application, as shown in Fig. 12.

4.5 3D garment virtual try-on

In this experiment, we perform a dynamic virtual try-on of the 3D garment on the virtual 3D models for the reconstructed six 3D garment models.

The physical force modelling is applied for 3D garment virtual try-on. 3D garment physical force modelling exploits the mechanical principles of 3D garment meshes, which converts the 3D garment meshes into 3D garment physical models. The 3D garment physical models can be affected by external and internal forces during the processing of virtual fitting. External forces consist of gravity and wind forces. Internal forces are the interaction forces between mesh vertices. Once 3D garment physical models are achieved, the dynamic simulation of the virtual try-on is applied to update positions of all vertices by the sum of in-plane membrane and outplane bending energies, as illustrated by (13).

$$W(x) = W_M(x) + W_B(x) \tag{13}$$

$$W_M(x) = k_M \sum (1 - \left\|\vec{x}_{ij}\right\| / \left\|\vec{u}_{ij}\right\|)^2 \left\|\vec{u}_{ij}\right\| \tag{14}$$

$$W_B(x) = k_B \sum (\theta_{ij}/\bar{\theta}_{ij})^2 \left\|\bar{\theta}_{ij}\right\| \tag{15}$$

Fig. 12 Comparison between the real-life original garment and the 3D garment mesh reconstructed by rolling ball method

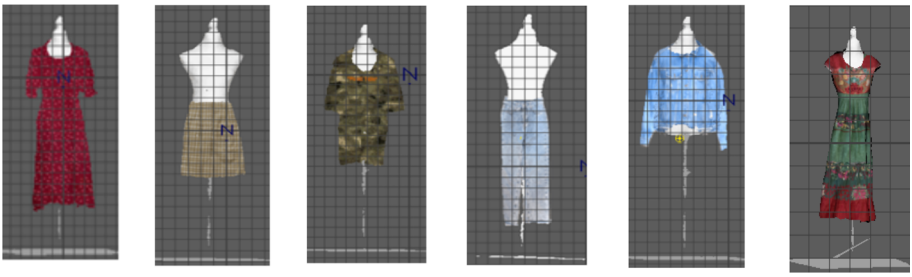

Fig. 13 The results of a virtual try-on experiment on the initial model

where $W_{M(x)}$ is the membrane energy as a summation over lengths of edges. $W_{B(x)}$ is the discrete bending energy as a summation over mesh edges with the corresponding dihedral angle. k_M and k_B are stretch and bending stiffness coefficients, respectively. We refer readers to our paper [42] for more detailed information about the dynamic simulation.

When simulating dynamic virtual fitting of 3D garment models, a physical model is generated through a spring-mass model to form the garment fabric. This is achieved by setting parameters such as collision thickness, collision strength, collision range, mass, tensile resistance, damping, and wind speed. The collision thickness is set to 0.071, the collision strength is set to 1.0, the collision range is set to 1.785, the mass is set to 1.0, the damping is set to 1.484, the tensile resistance is set to 50.549, and the wind speed is set to 10. The evaluation metric for virtual try-on is the fit of the garment model on the human body. The deformed garment model can achieve a smooth and flat fit on the chest, waist, and buttocks of the human body structure, ensuring moderate relaxation and avoiding penetration.

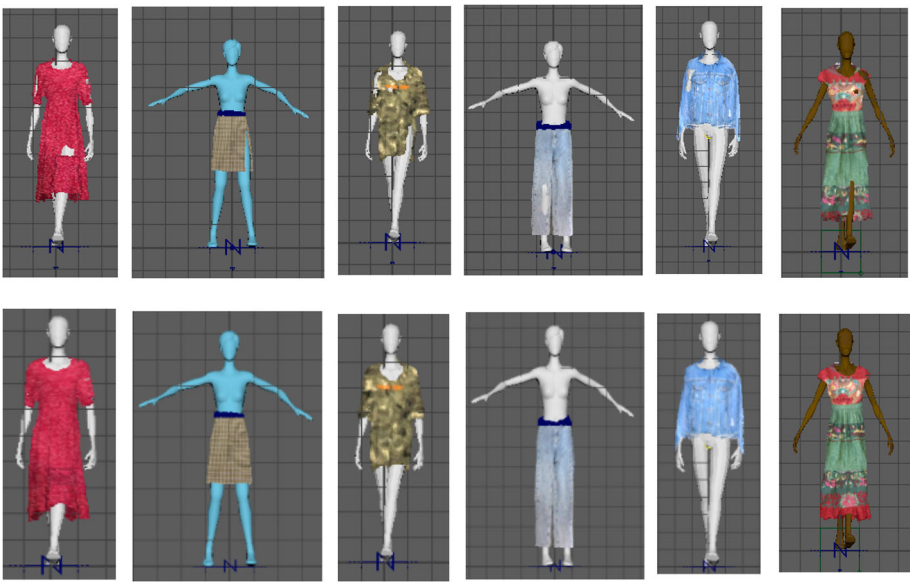

Fig. 14 The results of the model's try-on in different poses show the experimental results before and after the try-on

Fig. 15 The figure shows an experimental comparison between real-life garments and virtual try-on effects

Finally, we add textures to the 3D garment models and show the comparison results before and after the try-on in Figs. 13 and 14.

We conducted an experimental comparison between real-life garments and virtual try-on effects, using dresses and red dots as examples in Fig. 15. Noting that the difference in cm in Table 6 is due to the body size changes in the virtual model, rather than the construction accuracy. As the 3D model size changes (e.g., such as the size of bust, waist, and hips), the reconstructed 3D garment mesh also undergoes corresponding deformations in terms of dress length, waist, bust, and shoulder width to fit the body size and shape as shown in Tables 6 and 7. More importantly, using a denim jacket and red dots dress as examples, we have shown that our proposed framework is capable of adding different fabric properties, textures and physical behaviours to the virtual try-on garment models, showcasing the rich diversity of various garments that our system can handle also in terms of also adapting to different human models as shown in Fig. 16.

In conclusion, the comparison results show that our framework outperforms COLMAP on 3D point cloud garment reconstruction. The proposed segmentation and de-noising module separates the complex 3D background and the 3D garments from the 3D scene, and also removes the noise and the outliers for the 3D garment point clouds. Finally, the virtual try-on experiments show that our framework obtains high-quality and realistic 3D garment meshes to fit different body shapes.

5 Conclusion

In this paper, we have presented a novel computer-vision reconstruction framework for reconstructing high-quality realistic 3D digital garments. The proposed framework consists of three main modules including a 3D point cloud extraction module, a 3D point cloud segmenta-

Table 6 Comparison between real-life garments and virtual try-on effects

Dresses	Skirt length(cm)	waist(cm)	Bust(cm)	Shoulder width(cm)
Real-life original	4.88	1.08	1.27	1.62
Virtual try-on	4.37	0.99	1.06	1.32

Table 7 Comparison between real-life garments and virtual try-on effects

Red dots	Skirt length(cm)	Waist(cm)	Bust(cm)	Shoulder width(cm)
Real-life original	4.92	1.15	1.37	1.84
Virtual try-on	4.79	1.13	1.08	1.65

tion and de-noising module, and a mesh surface reconstruction and virtual try-on module. The comparison results show that our framework outperforms COLMAP on 3D point cloud garment reconstruction and provides realistic 3D garment meshes for the 3D virtual try-on comparing it with greedy projection triangulation and Poisson reconstruction on 3D garment mesh reconstruction. Finally, the 3D virtual try-on experiment shows that our framework fits different 3D human models with different 3D garment sizes. Our framework also has great potential for garment future technology, such as online garment shopping, garment design and manufacturing.

It is worth mentioning that the quality of 3D reconstruction by our framework can be affected by low-light conditions, complex backgrounds, and dramatic fabric deformations. Thus, we aim to address these challenges in future work through further optimizing triangulation methods and beam adjustment algorithms, making these methods to be adaptive to complex environmental conditions. To explore the deep learning 3D segmentation methods and mesh reconstruction, currently, there is a lack of available garment point cloud datasets for deep learning training. It also has the potential to further explore the use of edge computing or GPU acceleration to enhance processing speed and enable interactive user experiences.

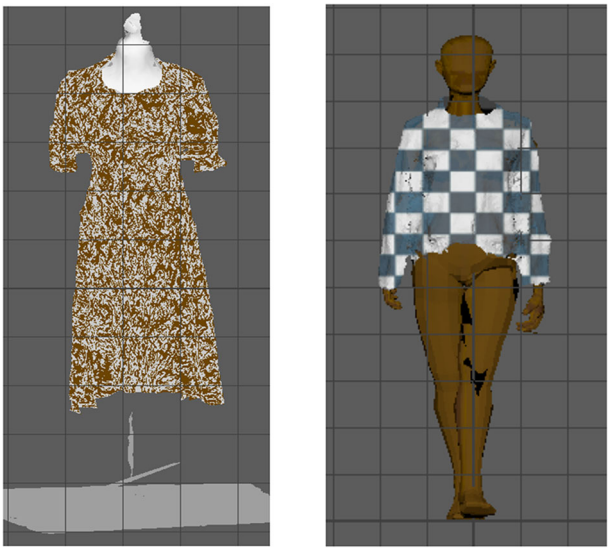

Fig. 16 The figure shows the experimental results of adding various textures to different garment models in virtual try-on

Acknowledgements This research did not receive any specific grant from funding agencies in the public, commercial, or not-for-profit sectors. Xi'an Major Scientific and Technological Achievements Transformation Industrialization Project, 23CGZHCYH0008.

Data Availability Data sharing is not applicable to this article as no datasets were generated or analysed during the current study.

Declarations

Conflicts of Interest The authors declare that they have no conflict of interest.

References

1. Bab-Hadiashar A, Gheissari N (2006) Range image segmentation using surface selection criterion. IEEE Trans Image Processi 15(7):2006–2018. https://doi.org/10.1109/TIP.2006.877064
2. Bernardini F, Mittleman J (1999) The ball-pivoting algorithm for surface reconstruction. Vis Comput Graph IEEE Trans 5(4):349–359
3. Brouet R, Sheffer A, Boissieux L (2012) Design preserving garment transfer. ACM Trans Graph 36:1–11. https://doi.org/10.1145/2185520.2185532
4. Chen J, Qin J, Zhong S, et al (2024) Sgm: a dataset for 3d garment reconstruction from single hand-drawn sketch. In: ICASSP 2024 - 2024 IEEE International Conference on Acoustics, Speech and Signal Processing (ICASSP) pp 2510–2514. https://doi.org/10.1109/ICASSP48485.2024.10447299
5. Chowdhury PN, Wang T, Ceylan D et al (2022) Garment ideation: Iterative view-aware sketch-based garment modeling. In: 2022 International conference on 3D vision (3DV). https://doi.org/10.1109/3DV57658.2022.00015
6. Cristovao C, Alessandro F, Vladimir K et al (2018) Nonlocality-reinforced convolutional neural networks for image denoising. IEEE Signal Processing Letters, pp 1–1. https://doi.org/10.1109/LSP.2018.2850222
7. Dik NY, Tsang WK, Chan AP, et al (2023) Analysing the effectiveness of a generative adversarial network model for the creation of new datasets of 3d human body and garment sizes in the clothing industry. Artificial Intelligence, Social Computing and Wearable Technologies 113(113)
8. El Hazzat S, Merras M (2023) Improvement of 3d reconstruction based on a new 3d point cloud filtering algorithm. Signal, Image Video Process 17(5):2573–2582
9. Eppstein B (1998) The crust and the b-skeleton: Combinatorial curve reconstruction. Graphical Models and Image Processing
10. Fang G (2013) Sketch-based garment pattern design. J Text Res 34(5):133–139
11. Fischler MA, Bolles RC (1981) Random sample consensus: a paradigm for model fitting with applications to image analysis and automated cartography. Commun ACM 24(6):381–395. https://doi.org/10.1145/358669.358692
12. Gálvez A, Iglesias A (2012) Particle swarm optimization for non-uniform rational b-spline surface reconstruction from clouds of 3d data points. Inf Sci 192(6):174–192
13. Guerrero P, Kleiman Y, Ovsjanikov M et al (2017) Pcpnet learning local shape properties from raw point clouds. Comput Graph Forum 37(2). https://doi.org/10.1111/cgf.13343
14. Gundogdu E, Constantin V, Seifoddini A et al (2018) Garnet: a two-stream network for fast and accurate 3d cloth draping. In: Proceedings of the IEEE/CVF international conference on computer vision pp 8739–8748. https://doi.org/10.1016/j.petrol.2018.02.070

15. von Hansen W, Michaelsen E, Thonnessen U (2006) Cluster analysis and priority sorting in huge point clouds for building reconstruction. In: 18th International Conference on Pattern Recognition (ICPR'06), vol 1, pp 23–26. https://doi.org/10.1109/ICPR.2006.1197
16. He Y, Xie H, Kazunori M (2023) Sketch2cloth: sketch-based 3d garment generation with unsigned distance fields. 2023 Nicograph International (NicoInt), pp 38–45. https://doi.org/10.1109/NICOINT59725.2023.00016
17. Hoppe H (2008) Poisson surface reconstruction and its applications. Acm Symposium on Solid and Physical Modeling
18. Hou G, Qin G, Yanhua L (2024) Self-supervised point cloud denoising method based on downsampling. J Jilin Univ Sci Ed 62(1):100–0105. https://doi.org/10.1109/ICASSP48485.2024.10447299
19. Hu H, Wang Q, Lu J (2023) Mspoint: point cloud denoising network based on multiscale distribution score. Laser & Optoelectron Prog 60(16):1615,002–1615,002. https://doi.org/10.3788/LOP222402
20. Hu TP Komura (2017) 3d textile reconstruction based on kinectfusion and synthesized texture. International Journal of Clothing Science and Technology 29(6). https://doi.org/10.1108/IJCST-01-2017-0007
21. Hu X, Zeng X, Liu J, et al (2020) Research and implementation of 3d reconstruction algorithm for multi-angle monocular garment image. In: 2020 IEEE International Conference on Artificial Intelligence and Computer Applications (ICAICA), pp 1068–1072. https://doi.org/10.1109/ICAICA50127.2020.9182424
22. Hwang C, Zhang L (2020) Innovative sustainable apparel design: application of cad and redesign process. Sustainability in the textile and apparel industries, pp 87–107. https://doi.org/10.13475/j.fzxb.20200505706
23. Jia J, Tang CK (2004) Inference of segmented color and texture description by tensor voting. IEEE Trans Pattern Anal Mach Intell 26(6):771–786. https://doi.org/2004.10.1109/TPAMI.2004.10
24. Kazhdan M, Hoppe H (2013) Screened poisson surface reconstruction. ACM Trans Graph (ToG) 32(3):1–13
25. Kuzmichev V, Moskvin aMA. (2018) Research on 3d reconstruction of late victorian riding skirts. Int J Cloth Sci Technol 30(6). https://doi.org/10.1108/IJCST-12-2017-0192
26. Liu K, Zeng X, Tao X et al (2021) Associate design of fashion sketch and pattern. IEEE Access 7:48,830–48,837. https://doi.org/10.1109/ACCESS.2019.2906261
27. Liu Z, Hu H, Lin Y et al (2022) Swin transformer v2: scaling up capacity and resolution. In: Proceedings of the IEEE/CVF conference on computer vision and pattern recognition, pp 12,009–12,019
28. Ma D (2017) Precise processing of point cloud data in omni-directional scanning based on three-dimensional laser sensor. J Nanoelectron Optoelectron 12(9):940–944. https://doi.org/10.1166/jno.2017.2216
29. Marco Centin, Alberto et al (2017) Mesh denoising with (geo)metric fidelity. IEEE Transactions on Visualization and Computer Graphics. https://doi.org/10.1109/TVCG.2017.2731771
30. Maurya SR, Magar GM (2018) Performance of greedy triangulation algorithm on reconstruction of coastal dune surface. In: 2018 3rd International conference for convergence in technology (I2CT) pp 1–6. https://doi.org/10.1109/I2CT.2018.8529765
31. Meier C, Berriel IS, Nava (2021) Creation of a virtual museum for the dissemination of 3d models of historical clothing. Sustainability 13(22):12,581. https://doi.org/10.1016/j.culher.2009.02.006.
32. Meng Y, Mok PY, Jin X (2010) Interactive virtual try-on clothing design systems. Comput Aided Des (4):310–321. https://doi.org/CNKI:SUN:SFXK.0.2019-03-015
33. Morelli L, Ioli F, Beber R et al (2023) Colmap-slam: a framework for visual odometry. Int Arch Photogramm Remote Sens Spat Inf Sci 48:317–324
34. Nyimbili PH, Demirel H, Seker DZ, et al (2016) Structure from motion (sfm)-approaches and applications. In: Proceedings of the international scientific conference on applied sciences, Antalya, Turkey, pp 27–30
35. PAN B, ZHONG Y (2020) Image-based three-dimensional garment reconstruction. J Text Res 41(4):123–128. https://doi.org/10.13475/j.fzxb.20190600806
36. Špelic I (2020) The current status on 3d scanning and cad/cam applications in textile research. Int J Cloth Sci Technol 32(6). https://doi.org/10.1108/IJCST-07-2018-0094
37. Qi CR, Su H, Mo K et al (2017a) Pointnet: deep learning on point sets for 3d classification and segmentation. In: Proceedings of the IEEE conference on computer vision and pattern recognition pp 652–660
38. Qi CR, Yi L, Su H, et al (2017b) Pointnet++: deep hierarchical feature learning on point sets in a metric space. Advances in Neural Information Processing Systems 30
39. Rakotosaona MJ, Barbera VL, Guerrero P et al (2019) Pointcleannet: learning to denoise and remove outliers from dense point clouds. Comput Graph Forum. https://doi.org/10.1111/cgf.13753
40. Rusu RB, Cousins S (2011) 3d is here: point cloud library (pcl). In: 2011 IEEE international conference on robotics and automation, pp 1–4. https://doi.org/10.1109/ICRA.2011.5980567
41. Stergiou M, Vosinakis S (2022) Exploring costume-avatar interaction in digital dance experiences. Exploring costume-avatar interaction in digital dance experiences. https://doi.org/10.1145/3537972.3537980

42. Tang W, Wan TR, Huang D (2016) Interactive thin elastic materials. Comput Anim Virt Worlds 27:141–150
43. Tian H, Zhu C, Shi Y et al (2023) Superudf: self-supervised udf estimation for surface reconstruction. IEEE Transactions on visualization and computer graphics. pp 1–11. https://doi.org/10.1109/TVCG.2023.3318085
44. Tian Q, Bai R, li D (2017) Point cloud segmentation of scattered artifacts based on improved euclidean clustering. Laser and Optoelectronics Exhibition 54(12):9
45. Trevor AJ, Gedikli S, Rusu RB et al (2013) Efficient organized point cloud segmentation with connected components. In: Proceedings of semantic perception mapping and exploration, pp 1–6
46. Umetani N, Igarashi DMKT (2011) Sensitive couture for interactive garment modeling and editing. ACM Trans Graph 30:1–12. https://doi.org/10.1145/2010324.1964985
47. Wang X, Wu L, Chen H (2020) Denoising of scattered point cloud data based on normal vector distance classification. J Jilin Univ (EngTechnol Ed) 50(1):278–288
48. Wenbo W, Yanchao Z, Xiangli W (2016) Pulsar signal denoising method based on laplace distribution in no-subsampling wavelet packet domain. Astron J 152(5):131. https://doi.org/10.3847/0004-6256/152/5/131
49. Wibowo A, Sakamoto D, Mitani J et al (2012) Dressup: a 3d interface for clothing design with a physical mannequin. In: Proceedings of the sixth international conference on tangible, embedded and embodied interaction, pp 99–102. https://doi.org/10.13475/j.fzxb.20190604406
50. Xiao D, Shi Z, Li S et al (2023) Point normal orientation and surface reconstruction by incorporating isovalue constraints to poisson equation. Comput Aided Geom Des 103(102):195. https://doi.org/10.1016/j.cagd.2023.102195
51. Xu PJ, Mok Y (2016) A web-based design support system for fashion technical sketches. Int J Cloth Sci Technol 28(1). https://doi.org/10.1108/IJCST-03-2015-0042
52. Yan J (2018) Research and implementation of 3d clothing modeling algorithm. Zhejiang University. https://doi.org/CNKI:CDMD:2.1018.259507
53. Yasseen Z, Nasri A, Boukaram W et al (2013) Sketch-based garment design with quad meshes. Comput-Aided Des 45(2):562–567
54. Yu X, Wang J, Yu L (2017) Inheritance and application of traditional culture in game clothing under the background of digital art. In: 3rd International conference on arts, design and contemporary education (ICADCE 2017) pp 481–484. https://doi.org/10.3969/j.issn.1003-8388.2016.01.011
55. Zengbo. WQX, Si Y (2021) 3d garment model reconstruction based on scattered point cloud. Journal of Physics: Conference Series 1790(1):012,090–. https://doi.org/10.1088/1742-6596/1790/1/012090
56. Zhou Y, Wang et al (2014) A fast and accurate segmentation method for ordered lidar point cloud of large-scale scenes. IEEE Geosci Remote Sens Lett 11(11):1981–1985. https://doi.org/10.1109/LGRS.2014.2316009
57. Zhou K, Xu Z (2023) Three-dimensional human dimension measurement based on multi-view virtual modeling. Modeling and simulation. https://doi.org/10.12677/MOS.2023.123227
58. Zhou Y, Wang D, Xie X et al (2014) A fast and accurate segmentation method for ordered lidar point cloud of large-scale scenes. IEEE Geosci Remote Sens Lett 11(11):1981–1985. https://doi.org/10.1109/LGRS.2014.2316009
59. Zhouyan L (2018) Key techniques of complex object surface modeling based on point cloud. Shandong University of Science and Technology